Available online www.jocpr.com

Journal of Chemical and Pharmaceutical Research, 2017, 9(8):29-33

Research Article

ISSN : 0975-7384
CODEN(USA) : JCPRC5

The Magnetic Properties of Alpha Phase for Iron Oxide NPs that Prepared from its Salt by Novel Photolysis Method

Zaid Hamid Mahmoud*

Department of Chemistry, Collage of Science, Diyala University, Diyala, Iraq

---

ABSTRACT

The present article was studied a novel and effective method to fibrate alpha phase of iron oxide NPs using photolysis method. The identity, structure, and size of particles were evaluated using XRD, TEM, while the spectra properties of it characterized using FTIR and UV-Vis as well as magnetic properties of alpha phase, was gauged using SQUID and showed deflection between FC and ZFC under Tirr=104 K. The magnetization curve of ZFC obtained the maximum value at TB=51 K and it didn't offer the Morin transition. SPION was obtained from M (H) at 300 K and the data of M (H) determined by Langevin function. Moreover, high magnetization was shown at 25°C (Ms=3.98 eum/g) and this eligible for biomedicine application.

Keywords: Photolysis; Novel; Hematite; Nanoparticles; Cooled field; Zero cooled field

---

INTRODUCTION

Through the diverse nanomaterials, the oxide of materials such iron oxide are the remarkable category of materials that have optical, electrical and magnetic properties which apply to the wide range [1] such as electrode materials, environmental pollutant clean up agent, pigment, catalyst and magnetic materials [2-5]. With a view to realizing usable properties, compilation conditions must be fully controlled to gain all powders together with a cramped particle size distribution and the desired crystallinity of the particles. The more steady of iron oxide is hematite and it has important properties such as environmentally friendly, non-toxic, low cost and high impedance to corrosion and it crystallized in rhombohedral lattice system with R-3C space group, n-type semiconducting properties and band gap equal to 2.1 eV [2]. Many methods are used to prepare nanoparticles of hematite as precipitation, sol gel, hydrothermal, microwave, precipitation from anhydrous, sonochemical methods and others [6-10]. This research focuses on the new method to prepare using UV irradiation that emitted from the system which contains from source with 125 watt and cooled system to avoid high temperature and it method contains two steps: the first is irradiate the solution of salt to produce oxy-hydroxide then burned it at high temperature. Compare with other methods, photolysis method has important properties such economy, don't have high energy, gain low particles and high purity. Many scientific sets in over the last few years have devoted to promoting and improving the magnetic properties of nanomaterial depending on Neel temperature [11-22]. Neel temperature in hematite appear at 960 K while at 263 K Morin temperature take place and below this temperature, the hematite is an antiferromagnetic whereas ferromagnetic above it [2]. When the particle size of materials decreases, the Morin and Neel temperatures are reduced and vanish [23,24]. The small particle size of hematite is appear superparamagnetic behavior above blocking temperature and ferromagnetic below it. Consequently, the nanoparticle is an entertaining for essential research of magnetic properties, due to it can show superparamagnetic, anti and weak ferromagnetic properties [25-27].

EXPERIMENTAL SECTION

Hematite NPs Fabricate

The alpha phase of iron oxide was fabricated using the system of irradiation with 125 watts as an irradiated source. First, 0.01 mole of $FeCl_3.6H_2O$ was dissolved in 100 ml distilled water to prepare the clear solution. Then, it was irradiated under the cooling system to avoid temperature that produces from the source until a precipitate formed. After that, the precipitate was isolated and washed with acetone for several times and dried. The final precipitate was burned at 400°C for 2 h to gain brown precipitate with magnetic properties.

Hematite NPs Characterization

FTIR (65-FT-IR, Perkin Elmer, USA) and UV-Vis spectrophotometer (JASCO Asia Portal UV-visible model V-650) were used to determine the functional group and energy gap of powder respectively while the size of particles and the identity of it was showed using TEM (JEOL JEM -2100) and XRD spectrum (Shimadzu-XRD-6000) with Cu Kα radiation respectively and the magnetic properties of it was determined using Commercial Quantum Design MPMS-XL-5.

RESULTS AND DISCUSSION

Many techniques were used to characterize the hematite NPs that prepared using photolysis such as FTIR, UV-Vis, XRD, TEM, and SQUID. FTIR spectrum of hematite NPs was recorded at room temperature and showed at Figure 1. In Figure 1, the characteristic Fe-O two sharp peaks appear at 478 and 568 cm^{-1} and the broad band appear at 3441 cm^{-1} back to O-H of water molecules [28,29].

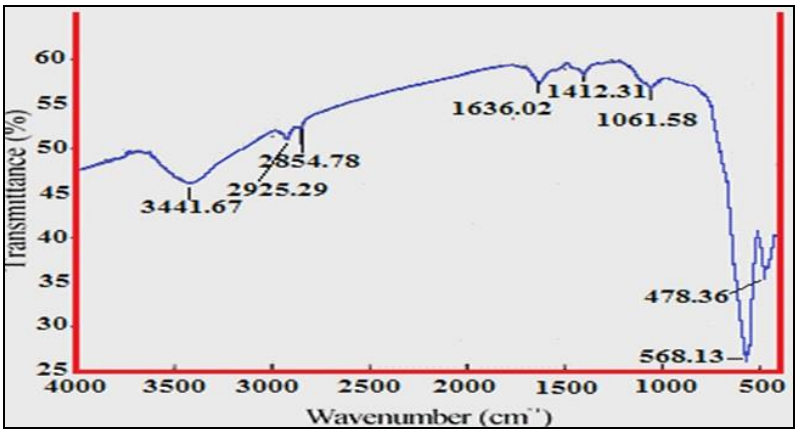

Figure 1: FTIR spectrum of hematite NPS

In region (425-725), NPs of hematite (Figure 2) appears an absorption band and it back to d-d transition and the transition between 2p for oxygen atom to 4s for the iron atom [30,31]. The value of energy gap for NPs was showed from below equation depending on λ the max of adsorption and equal to 2.45.

$$Eg=1240/\lambda \text{ max} \quad (1)\ [32]$$

The XRD spectrum of NPs of hematite was obtained at Figure 3 and all patterns or diffraction peaks indicate to the alpha phase of iron oxide and hexagonal structure which is in good agreement with a card (86-0550). The sharps peaks of alpha phase indicate that the structure of it highly crystalline and the average size of the particles were calculated using Debye-Scherrer equation as following:

$$D=0.9\lambda / \beta\text{Cos}\theta \quad (2)\ [33]$$

Which λ the x-ray wavelength, D: the size of particles, θ Bragg angle and β is the excess line boarding and it founded equally to 10 nm.

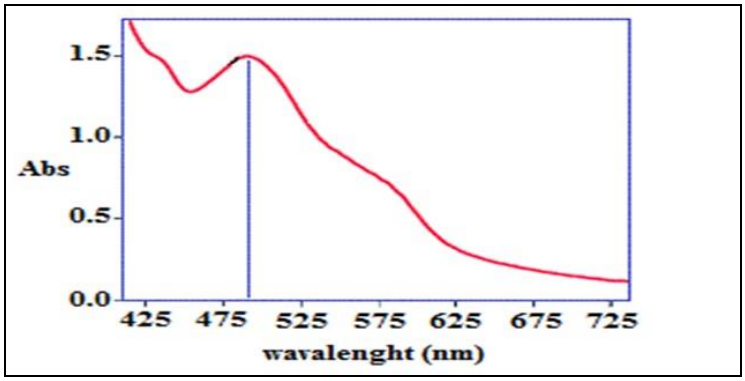

Figure 2: UV-Vis spectrum of hematite NPS

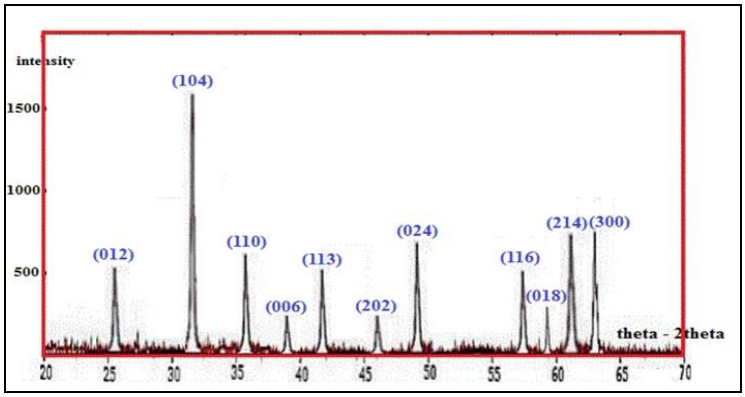

Figure 3: XRD spectrum of hematite NPs

The morphology and the size of particles were determined using TEM technology and showed at Figure 4. The result was obtained nanoparticles with narrow size and spherical morphology and the evaluated average size of NPs using TEM about 10 nm and the result is good agreement with XRD results.

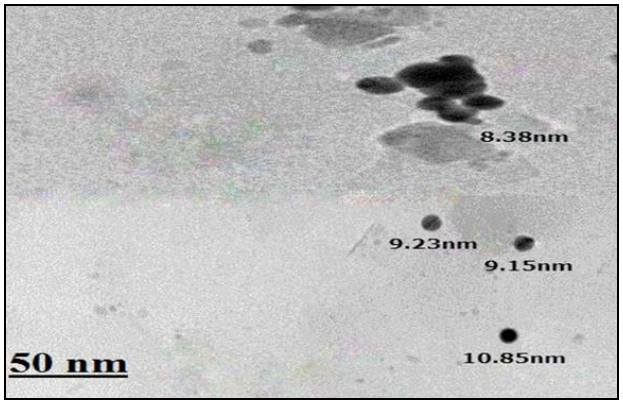

Figure 4: TEM of hematite NPs

Using (SQUID), the magnetic properties of hematite NPs were measured and applied low magnetic field about 100 Oe. The curves of ZFC (zero fields cooled) and FC (felid cooled) was measured and obtained at Figure 5. For ZFC magnetization, the sample cooled to 5 K in the obscurity field of magnetic and the finite field that applied equal 100 Oe then the sample heat up to 300 K and the measuring of magnetization continuous while for FC, the sample was cooled to 5 K under the same finite field. All data was showed at

Figure 5 under the heat up of the sample to 300 K and it saw the magnetization behavior of NPs and according to Figure 5 the ZFC magnetization decreased and FC increased below blocking temperature.

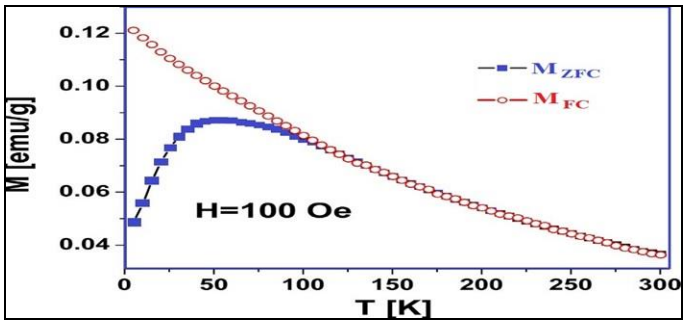

Figure 5: The curves of FC and ZFC at H= 100 Oe

The behavior of FC is generally counted to be feature magnetic for NPs with no interactions between the particles [34,35]. The rise in the curve of FC magnetization under blocking temperature indicated to found strong interaction inter between the particles [36]. The Tirr (irreversible temperature) that found in FC and ZFC curves begin to detach corresponds to TB of the largest in the system. A point which the ratio of MFC-MZFC/MFC less than 1%, the Tirr determined and this gauge gives a value at 104 K and between difference Tirr and TB, it can review the distribution of NPs and equal to 51, thus pointing a not wide size distribution for the particles. As predictable for the particles, the NPs of hematite weren't displaying the Morin temperature [37]. The (M(H)) (magnetization against applied magnetics field) isn't hysteretic at 300 K (Mr=0 emu/g and MC=0 Oe), as predictable in the unblocked regime over Tirr at Figure 6 and by using Langevin theory, the superparamagnetic state was described and gives as the following equation:

$$M(H,T) = M_s[\text{Coth}\frac{m_pH}{K_BT} - \frac{K_BT}{m_pT}] \quad (3)$$

Where: H indicates the applied magnetic field, m_p: the magnetic momentum of NPs. Figure 6 was obtained the data of M(H) at 300 K. The best parameter showed at m_p=657 MB, M_s=3.98 emu/g and these indicate the average of NPs equal to 10 nm according to the following equation:

$$m_p = \frac{\pi d^3 M_s}{6} \quad (4)$$

This value was found using Langevin theory [38] and in agreement with the result from XRD and TEM.

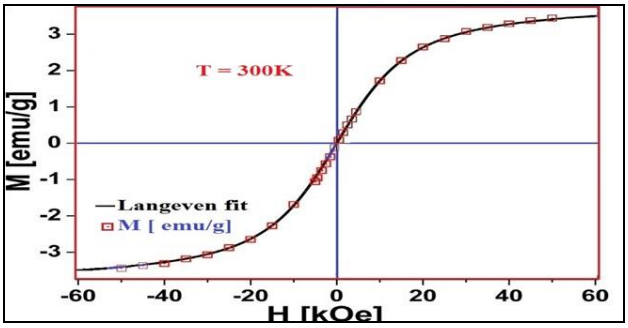

Figure 6: Magnetization against applied magnetics field at 300 K

CONCLUSION

We successfully fabricated alpha phase of iron oxide NPs with magnetic properties using photolysis method. Hematite phase with spherically shaped morphology and the average size about 10 nm was revealed using XRD and TEM. At blocking and irreversible temperatures equal to 51 and 104 K respectively, NPs of hematite appeared superparamagnetic properties and under 5 K, it didn't offer Morin transition. From Langevin's curve, the results of M(H) was successfully fitted in it and the average size of particles that obtained from fit was in agreement with XRD and TEM results as well as it found the M_s equal 3.98 emu/g and 657 for M_p.

REFERENCES

[1] L Zhou; J Xu; X Li; F Wang. *Mat Chem Phys*. **2006**, 97, 137.
[2] A Teja; P Koh. *Progress in Crystal Growth and Characterization of Materials*. **2009**, 55, 22–45.
[3] M Huang. *Ceram Int*. **2014**, 40, 10537–10544.
[4] H Liang; W Chen; Y Yao; Z Wang; Y Yang. *Ceram Int*. **2014**, 40, 10283–10290.
[5] M Khalil; J Yu; N Liu; RL Lee. *Surf A: Physicochemical Eng Aspects*. **2014**, 453, 7–12.
[6] P Tartaj, M Morales, S Veintemillas-Verdaguer, T Gonzalez-Carreno, CJ Serna. Handbook of Magnetic Materials; Elsevier: Amsterdam, the Netherlands. **2006**, 403.
[7] M Crişan; A Brăileanu; M Răileanu; D Zaharescu; M Crişan; N Drăgan; M Anastasescu; A Ianculescu; I Niţoi; VE Marinescu; SM Hodorogea. *J Non Crystalline Solids*. **2008**, 354, 705–711.
[8] D Makovec; A Kosak; A Znidarsic; M Drofenik. *J Magn Mat*. **2005**, 289, 32-35.
[9] J Rockenberger; EC Scher; A Alivisatos. *J Am Chem Soc*. **1999**, 121, 11595-11596.
[10] AB Chin; II Yaacob. *J Mater Process Technol.* **2007**, 191, 235-237.
[11] S Saravanakumar; R Saravanan; S Sasikumar. *Chem Pap*. **2014**, 68, 788–797.
[12] F Sánchez-DeJesús; AM Bolarín-Miró; CA Cortés-Escobedo; R Valenzuela; S Ammar. *Ceram Int*. **2014**, l40, 4033–4038.
[13] A Zelenakova; V Zelenak; S Michalik; J Kovac; MW Meisel. *Rev Phys B*. **2014**, 89, 104417.
[14] SI SrikrishnaRamya; CK Mahadevan. *Solid State Chem.* **2014**, 211, 37–50.
[15] H Liang; X Xu; WB Chen; Z Wang. *Cryst Eng Comm*. **2014**, 16, 959–963.
[16] V Panchal; U Bhandarkar; M Neergat; KG Suresh. *Appl Phys A.* **2014**, 114, 537–544.
[17] B David; N Pizurova; P Synek; V Kudrle; O Jasek; O Schneeweiss. *Mater Lett*. **2014**, 116, 370–373.
[18] D Peeters; G Carraro; CMaccato; H Parala; A Gasparotto; D Barreca; C Sada; K Kartaschew; M Havenith; D Rogalla; HWA Becker. *Phys Status Solidi A*. **2014**, 211, 316–322.
[19] A Zelenakova; V Zelenak; V Bednarcik; P Hrubovcak; J Kovac. *J Alloys Compd*. **2014**, 582, 483–490.
[20] B Vallina; JD Rodriguez-Blanco; AP Brown; LG Benning. *J Nanopart Res.* **2014**, 16, 2322.
[21] J André-Filho; L León-Félix; J Coaquira; V Garg; A Oliveira. *Hyperfine Interact*. **2014**, 224, 189–196.
[22] HI Adegoke; FA Adekola; OS Fatoki; BJ Ximba. *Korean J Chem Eng*. **2014**, 31, 142–154.
[23] M Tadic; V Kusigerski; D Markovic; I Milosevic; V Spasojevic. *J Magn Mater*. **2009**,321, 12–16.
[24] D Cardillo; M Tehei; M Lerch; S Corde; A Rosenfeld; K Konstantinov. *Mater Lett*. **2014**, 117, 279–282.
[25] M Tadic; N Citakovic; M Panjan; Z Stojanovic; D Markovic; V Spasojevic. *J Alloys Compd*. **2011**, 509, 7639-7644.
[26] M Tadic; N Citakovic; M Panjan; B Stanojevic; D Markovic; D Jovanovic; V Spasojevic. *J Alloys Compd*. **2012**, 543, 118–124.
[27] M Tadic; D Markovic; V Spasojevic; V Kusigerski; M Remskar; J Pirnat; Z Jaglicic. *J Alloys Compd*. **2007**, 441, 291–296.
[28] H Deligöz; A Baykal; E Tanriverdi; Z Durmus. *Mater Res Bull*. **2012**, 47, 537.
[29] G Gao; P Huang; Y Zhang; K Wang; W Qin; X Cui. *Cryst Eng Comm*. **2011**, 13, 1782.
[30] DM Sherman; TD Waite. *Am Mineral*. **1985**, 70, 1262.
[31] DM Sherman. *Phys Chem Miner*. **1985**, 12, 161.
[32] M Geetha; K Suguna; P Anbarasan; V Aroulmoji. *Int J Adv Sci Engg*. **2014**, 1(1), 1-5.
[33] M Ahmad; A Rahdar; F Sadeghfar; S Bagheri; MR Hajinezhad. *Nanomed Res J*. **2014**, 1, 39-46.
[34] K Mohammadikish. *Ceram Int*. **2014**, 40, 1351–1358.
[35] H Yan; X Su; C Yang; J Wang; C Niu. *Ceram Int*. **2014**, 40, 1729–1733.
[36] Y Xu; X Rui; Y Fu; H Zhang. *Chem Phys Lett*. **2005**, 410, 36–38.
[37] A Ay; D Konuk; B Zümreoglu-Karan. *Nanoscale Res Lett.* **2011**, 6, 116.
[38] J Ma; K Chen. *Phys Status Solid RRL*. **2012**, 6, 324–326.